

The effect of the short wave radiation and its reflected components on the Mean Radiant Temperature: modelling and preliminary experimental results

Concettina Marino, Antonino Nucara, Matilde Pietrafesa, Erika Polimeni

Dipartimento di Ingegneria Civile, dell'Energia, dell'Ambiente e dei Materiali (DICEAM), "Mediterranea" University of Reggio Calabria, Via Graziella, Feo di Vito, 89122, Reggio Calabria, Italy

Abstract

In outdoor as well as indoor environments, human thermal sensation strongly depends on the direct component of solar radiation incident on the body. Nevertheless, even though the direct component exerts the major contribute on this issue, especially in indoor environments and confined spaces, the diffuse and reflected components of the solar radiation also affects the thermal sensations of people. Despite this evidence, simple and reliable methods designed to take into account the effect of solar radiation on the indoor radiant field enveloping the human being in indoor environments are hardly available.

This article aims to provide a contribute on this topic, proposing a model for the computation of the mean radiant temperature (MRT) in indoor environments in presence of solar radiation. The most innovative facet of the proposed model regards the computation of the effects of the radiation components reflected by the internal surfaces.

Moreover, in order to try a preliminary validation of the model, an experimental campaign was also carried out and MRT values were measured in positions either directly irradiated by the sun or shielded from direct irradiation. The purpose of the measurements was to preliminarily analyze the extent of the accuracy with which the model might predict the rise of MRT due to solar direct irradiation.

Keywords

Mean Radiant Temperature; Solar radiation; Indoor environment.

1 Introduction

In both outdoor and indoor environments, human thermal comfort is influenced by various factors (climate conditions, physiological and subjective issues, etc.), which have combined and

diversified effects on human energy balance. Comfort and energy demand in buildings are strongly interconnected and the achievement of high quality standards involves an energy cost, which must be taken into account [1–3]. The maintenance of the required environmental quality levels, as a matter of fact, implies that a series of environmental variables should be controlled within recommended values [4]; nevertheless, this approach could not suffice in many actual cases, when comfort indexes [5], parameters and variables should be accurately evaluated [6,7].

Among all these factors, radiative heat exchanges play a pivotal role: in confined environments they contribute as far as 30% of the whole thermal exchanges involving the subject [8], but in case of direct solar radiation they can become the most significant cause of heat gain and discomfort [9].

The mean radiant temperature, MRT, is one of the main factors used to quantify the effect of the radiant field on human thermal response [10]. This quantity plays a crucial role in both outdoor and indoor situations and several studies have stressed the influence of this variable on thermal comfort in urban settings [11], researching and comparing reliable and feasible methods for its assessment [12–14] or its measurement [15–18]. All these studies, moreover, consider solar radiation as a key factor in the assessment of the mean radiant temperature on the grounds that thermal comfort is highly dependent on both long wave and short wave radiation fluxes from the surroundings.

In indoor environments, the influence of the mean radiant temperature on thermal comfort is also well documented [19–23]. Moreover, in this case, MRT also influences the energy consumption to a certain extent. The issue has been investigated, analyzing the energy saving potential in a PMV-controlled space [24]. The results suggested that energy consumption, in a thermal comfort-controlled space, is strongly affected by a change in the mean radiant temperature and that the thermal comfort control can be considered as a reasonable strategy for both thermal comfort and energy saving purposes which, in turn, are to become one of the main objectives of the building industry all over the world [25–28]

On balance, the accurate assessment of radiant field and MRT is the key to achieving both comfort optimization and energy efficiency.

However, also in indoor environments, both radiant field and MRT are strongly affected by short wave and long wave radiation fluxes and several experimental analyses have demonstrated that solar radiation is a significant cause of discomfort to people [29].

Despite this evidence, there are few models [8,30,31] which allow analytical assessment of MRT taking into account solar radiation.

This article aims to provide a contribute on this topic, proposing a model for the computation of mean radiant temperature values, in thermal moderate indoor environments, in the presence of solar radiation. The most innovative facet of the proposed model regards the computation of the effects of the radiation components reflected by the indoor surfaces. Indeed, considering the various surfaces which, by and large, the building envelope is composed of, these components might have a considerable influence on MRT.

In order to further investigate on this subject, an experimental campaign was also carried out using the globe-thermometer method and MRT values were measured in positions directly irradiated by the sun or shielded from direct irradiation.

2 The calculation of the mean radiant temperature of a subject exposed to solar radiation: the proposed model

The proposed model is aimed at the calculation of the mean radiant temperature (\bar{T}_r) inside an indoor environment when the human subject is exposed to direct, diffuse and reflected solar radiation.

It considers the human body totally surrounded by an enclosed environment, so that, in this condition, if only radiative thermal exchange are taken into account, the net flux leaving the human body (Q_S) is equal to the flux exchanged for radiation among the human body and the surfaces of the environment ($Q_{E \leftrightarrow S}$) which the subject is in. That is [8,32]:

$$Q_{E \leftrightarrow S} = Q_S \quad (1)$$

According to the MRT definition (which is the uniform temperature of an enclosure where the radiative flux on the subject, is the same as in the actual environment [33]), it is now assumed that the environment is an enclosure with a uniform temperature \bar{T}_r ; it is also assumed that the temperature of the human body is equal to the mean temperature of its clothed surface, T_{cl} . In this case, the thermal radiative flow exchanged between a subject and the surrounding surfaces of the enclosed environment is given by [8,32]:

$$Q_{E \leftrightarrow S} = \frac{A_S \sigma (\bar{T}_{cl}^4 - \bar{T}_r^4)}{\frac{1}{\varepsilon_S} + \frac{A_S}{A_E} \left(\frac{1 - \varepsilon_E}{\varepsilon_E} \right)} \quad (2)$$

where $\sigma = 5.67 \times 10^{-8} \text{ W m}^{-2} \text{ K}^{-4}$ is the Stefan-Boltzman constant; ε_S and ε_E are the emissivities of the human body and of the surfaces of the environment respectively; A_S is the effective area of the

human body exposed to radiation (i.e. the area of the smallest convex surface that contains the body); A_E is the whole area of the surfaces composing the environment envelope.

Provided that the subject is supposed to be much smaller than the surrounding environment, the ratio A_S/A_E can be neglected; in this case, the equation can be written as:

$$Q_{E \leftrightarrow S} = A_S \varepsilon_S \sigma (T_{cl}^4 - \bar{T}_r^4) \quad (3)$$

As far as the net flux Q_S is concerned, it is the net radiative energy lost by the human body and, therefore, it can be evaluated as the difference among the emitted flow, Q_{0S} , and the absorbed share of the thermal flow, $Q_{S,abs}$, that reaches the subject. That is:

$$Q_S = Q_{0S} - Q_{S,abs} \quad (4)$$

where, in turn, the long wave radiation energy emitted by the human body, Q_{0S} (Figure 1), can be assessed with the well-known equation:

$$Q_{0S} = A_S \varepsilon_S \sigma T_{cl}^4 \quad (5)$$

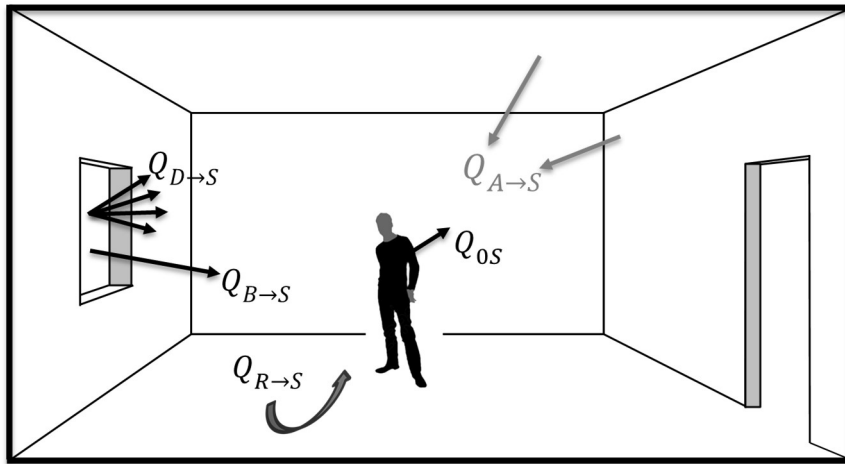


Figure 1 – Radiative exchanges between the environment and the human body.

When the sun is not involved in the radiative exchanges, $Q_{S,abs}$ is only due to the radiative flux emitted by the surfaces of the environment ($Q_{A \rightarrow S}$), but, when the sun enters the indoor environment which the subject is in, its contribute to $Q_{S,abs}$ can not be neglected.

In this case, the following contributes to $Q_{S,abs}$ can be pointed out (Figure 1 and Figure 2):

- the long wave radiation energy emitted by the surfaces of the environment and received by the subject, $Q_{A \rightarrow S}$;
- the short wave solar radiant flux on the body surface, due to the diffuse sky radiation entering the room through the glazed surface, $Q_{D \rightarrow S}$;

- the short wave solar radiant flux on the body surface, due to the direct radiation entering the room through the glazed surface, $Q_{B \rightarrow S}$;
- the short wave solar radiant flux on the body surface due to the reflections of both direct and diffuse radiation on the environment surfaces, $Q_{R \rightarrow S}$

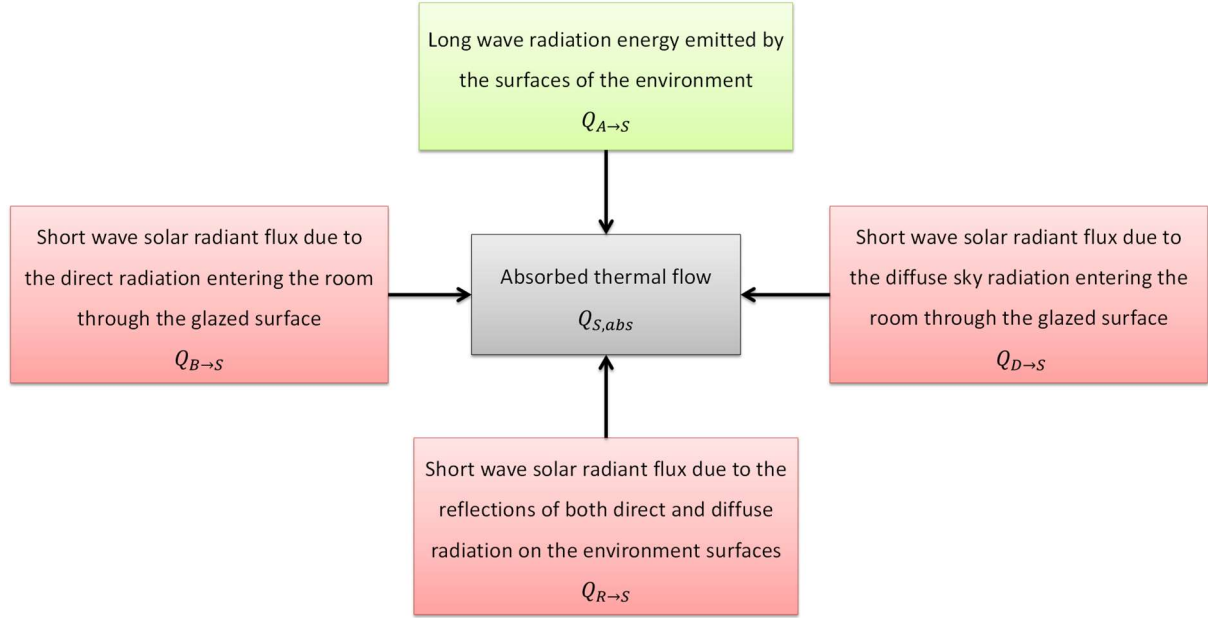


Figure 2 – Contributes to the absorbed share of the thermal flow, $Q_{S,abs}$, that reaches the subject.

Therefore, the absorbed share of the thermal flow, $Q_{S,abs}$, can be written as:

$$Q_{S,abs} = \alpha_{LW} Q_{A \rightarrow S} + \alpha_{SW} (Q_{D \rightarrow S} + Q_{B \rightarrow S} + Q_{R \rightarrow S}) \quad (6)$$

where α_{LW} is the long wave absorbance of the human body, equal to the emissivity $\varepsilon_s = 0.97$ [34], α_{SW} is the short wave absorbance and can be assumed equal to 0.7 [35].

2.1 Long wave radiation energy emitted by the surfaces of the environment and received by the subject

In the hypothesis that the internal surfaces of the building can be considered as black bodies, characterized by an emissivity $\varepsilon_i=1$ and a reflectance $\rho_i=1-\varepsilon_i=0$, the radiation coming from the surfaces of the indoor environment may be computed by means of the relationship:

$$Q_{A \rightarrow S} = \sigma A_S \sum_{i=1}^N F_{S \rightarrow i} T_i^4 \quad (7)$$

where $F_{S \rightarrow i}$ is the angle factor between the subject and the i^{th} surface of the envelope and T_i is the temperature of the i^{th} surface of the envelope.

Following the Fanger theory [34], the angle factor between the subject and the generic surface may be calculated under the hypothesis that the shape of the subject is taken into account by means of the projected area factors.

As a consequence, the angle factor is assessed by means of the following equation [34,36]:

$$F_{S \rightarrow i} = \int_{\frac{x}{y}=0}^{\frac{x}{y}=\frac{a}{c}} \int_{\frac{z}{y}=0}^{\frac{z}{y}=\frac{b}{c}} \frac{f_p}{\sqrt{\left[1 + \left(\frac{x}{y}\right)^2 + \left(\frac{z}{y}\right)^2\right]^3}} d\left(\frac{x}{y}\right) d\left(\frac{z}{y}\right) \quad (8)$$

where, with reference to Figure 3, a and b are the dimensions of the rectangular surface, c is distance between the subject and the same surface and $f_p = A_p/A_S$, assessable by means of the models reported in [34,37,38], is the projected area factor.

This latter characterizes the shape of the human body, depends on the posture of the subject, the azimuth, α , the altitude, β (Figure 3) and, therefore, it depends on the discretization used for singling out the surface dA in the numerical resolution of the integral.

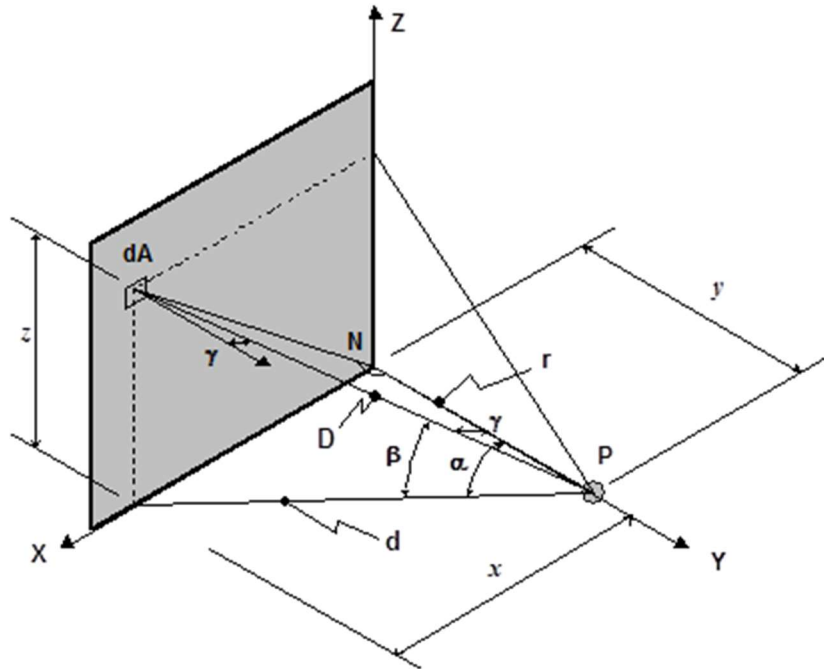


Figure 3 – Geometric parameters referring to the configuration of a subject facing a rectangular surface.

The angle factors may be also assessable by means of the algorithm reported in [36,39].

2.2 Short wave solar radiant flux on the body surface due to the diffuse radiation from the sky

In the hypothesis that the diffuse radiation entering the room through the glazed surfaces follows the Lambert's law [32,40], the solar radiation that reaches the subject can be evaluated by the following expression:

$$Q_{D \rightarrow S} = A_S \sum_{j=1}^{N_g} F_{S \rightarrow j} I_{dj} \quad (9)$$

where $F_{S \rightarrow j}$ is the angle factor between the subject and the j^{th} glazed surface of the envelope, I_{dj} is the diffuse sky radiation after crossing the j^{th} glazed surface, N_g the number of glazed surfaces. The calculation of the angle factors, which is of fundamental importance for the determination of this term, may be realized by means of some analytical or experimental methods [40,36,41].

2.3 Short wave solar radiant flux on the body surface due to the direct radiation

The contribution of the direct radiation to the human body's thermal balance is:

$$Q_{B \rightarrow S} = A_p I_b = f_p A_S I_b \quad (10)$$

where A_p is the projected area of the subject onto a plain normal to the direction of the solar beam, f_p is the projected area factor, and I_b is the direct radiation that strikes the subject.

2.4 Short wave solar radiant flux on the body surface due to the reflected radiation

When the short wave radiation (wavelength $< 2\mu\text{m}$) is considered, the hypothesis of black body behavior regarding the internal surfaces of the building is not feasible [35]; therefore the reflected component of the radiation should be taken into account.

Hereby, as regards the diffuse component, its reflection, $Q_{RD \rightarrow S}$, on the internal surfaces may be assessed as follows (Figure 4):

$$Q_{RD \rightarrow S} = \sum_{i=1}^N \rho_i \left(\sum_{j=1}^{N_g} A_j F_{j \rightarrow i} I_{dj} \right) F_{i \rightarrow S} \quad (11)$$

where N is the number of surfaces surrounding the subject, ρ_i is the reflectance of the i^{th} surface of the envelope, $F_{j \rightarrow i}$ is the angle factor between the j^{th} glazed surface and the i^{th} surface of the envelope.

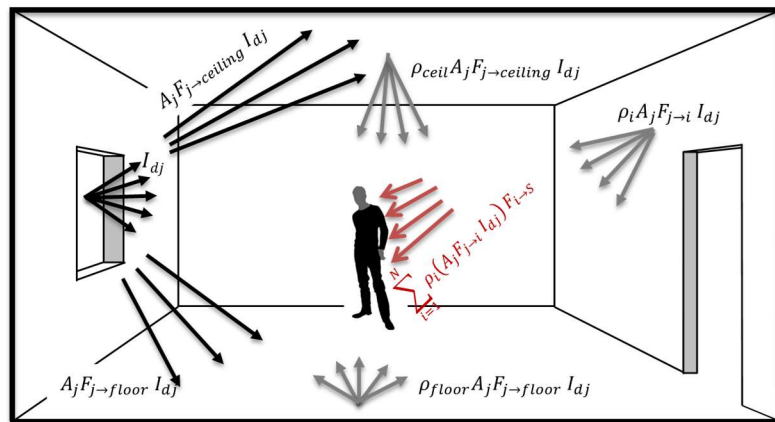


Figure 4 – Short wave solar radiant flux on the body surface due to the radiation diffuse from the sky, crossing the windows, and reflected by the interior walls.

Eq. (11), evidently, considers only the first reflection of the solar radiation on the opaque surfaces of the envelope, while assumes as negligible the effect of the multiple reflections among surfaces on the subject's thermal balance.

For the reciprocity relationship of the view factors:

$$F_{i \rightarrow S} = \frac{A_S F_{S \rightarrow i}}{A_i} \quad (12)$$

$$A_j F_{j \rightarrow i} = A_i F_{i \rightarrow j} \quad (13)$$

So that eq. (11) can be written as:

$$Q_{RD \rightarrow S} = A_S \left[\sum_{i=1}^N \rho_i \left(\sum_{j=1}^{N_g} F_{i \rightarrow j} I_{dj} \right) F_{S \rightarrow i} \right] \quad (14)$$

On the other hand, as far as direct radiation I_b is concerned, when it shines on the subject, also a portion of the floor surface is irradiated at least; if I_{bh} is the direct solar radiation on the horizontal plane and if the reflected radiation is assumed to be distributed on the lowest half of the exposed portion of the body [30], the contribute, $Q_{RB \rightarrow S}$, to the radiant flow investing the subject due to the floor reflections of the direct component (Figure 5) may be assessed as follows:

$$Q_{RB \rightarrow S} = 0,5 A_S \rho_{floor} I_{bh} \quad (15)$$

where ρ_{floor} is the reflectance of the pavement and I_{bh} is the direct radiation that strikes the horizontal surface of the pavement.

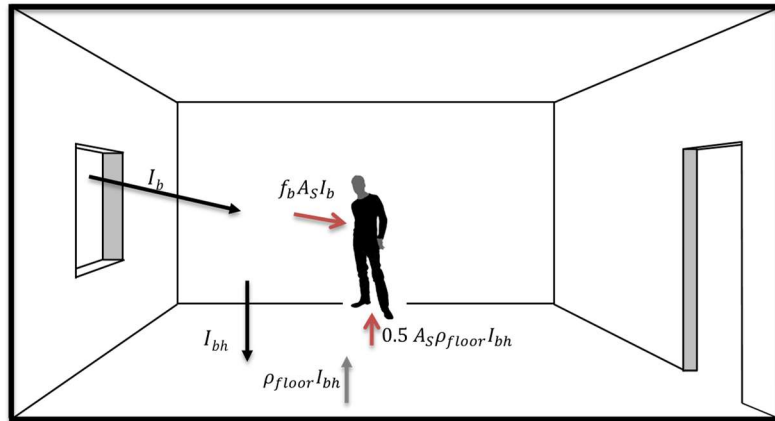


Figure 5 – Short wave solar radiant flux on the body surface due to the floor reflections of the direct component.

Following the indications reported in [30], ρ_{floor} , which, by and large, assumes the values of 0.3, can be increased up to 0.5, to take into account the effect of the long wave radiation generated by the local heating of the portion of the floor surface illuminated by the directed solar beam.

Finally, the contribution of the direct radiation to the human body's thermal balance is:

$$Q_{R \rightarrow S} = Q_{RD \rightarrow S} + Q_{RB \rightarrow S} = A_S \left[\sum_{i=1}^N \rho_i \left(\sum_{j=1}^{N_g} F_{i \rightarrow j} I_{dj} \right) F_{S \rightarrow i} + 0,5 \rho_{floor} I_{bh} \right] \quad (16)$$

2.5 Mean Radiant Temperature

By applying Eq. (1) and by utilizing Eqs. (3), (4) (5) and (6), we obtain:

$$A_S \varepsilon_S \sigma (T_{cl}^4 - \bar{T}_r^4) = A_S \varepsilon_S \sigma T_{cl}^4 - \alpha_{LW} Q_{A \rightarrow S} - \alpha_{SW} (Q_{D \rightarrow S} + Q_{B \rightarrow S} + Q_{R \rightarrow S}) \quad (17)$$

That yields:

$$\bar{T}_r = \sqrt[4]{\frac{\alpha_{LW} Q_{A \rightarrow S}}{A_S \varepsilon_S \sigma} + \frac{\alpha_{SW} (Q_{D \rightarrow S} + Q_{B \rightarrow S} + Q_{R \rightarrow S})}{A_S \varepsilon_S \sigma}} \quad (18)$$

Considering Eqs. (7), (8), (9) and (15) and assuming that, on the basis of Kirchoff's law, $\alpha_{LW} = \varepsilon_S$:

$$\bar{T}_r = \sqrt[4]{\sum_{i=1}^N F_{S \rightarrow i} T_i^4 + \frac{\alpha_{SW}}{\varepsilon_S \sigma} \left[\sum_{j=1}^{N_g} F_{S \rightarrow j} I_{dj} + f_p I_b + \sum_{i=1}^N \rho_i \left(\sum_{j=1}^{N_g} F_{i \rightarrow j} I_{dj} \right) F_{S \rightarrow i} + 0.5 \rho_{floor} I_{bh} \right]} \quad (19)$$

where $f_p = A_p/A_S$ is the projected area factor.

3 Preliminary experimental validation of the model

In this preliminary phase, the experimental measurements, carried out in the period July-August 2015, were designed in order to analyze the effect of the direct solar component on the mean radiant temperature and to validate the predictions of the proposed model in this regard. Specifically, the term $\Delta \bar{T}_{rb}^4 = \frac{\alpha_{SW}}{\varepsilon_S \sigma} (f_p I_b + 0.5 \rho_{floor} I_{bh})$ of eq. (18) is the object of the investigation.

In order to reach this aim, mean radiant temperature values were measured and compared with the ones calculated by means of the proposed method.

To measure the mean radiant temperature, the method of the globe-thermometer was used [33].

In this case the mean radiant temperature is assessed by means of the equation:

$$\bar{T}_{r,M} = \sqrt[4]{T_g^4 + \frac{h_{cg}}{\varepsilon_g \sigma} (T_g - T_a)} \quad (20)$$

where T_g and T_a are respectively the globe-thermometer and the air temperature, ε_g is the globe emissivity and h_{cg} is the convective heat transfer coefficient, which is assessed as the maximum of the two values calculated by means of the following equation:

$$h_{cg} = 1.4 \sqrt[4]{\frac{T_g - T_a}{D}} \quad (21)$$

$$h_{cg} = \frac{6.3 v_a^{0.6}}{D^{0.4}} \quad (22)$$

where D is the globe diameter (m) and v_a (m/s) is the air velocity.

The experimental campaign was structured on the basis of the following considerations: two globe-thermometers were used; the first one was located in a position directly irradiated by the sun, the second one was located as close as possible to the first one, but in a position not irradiated by the direct component of the solar radiation.

Consequently, two measured mean radiant temperatures were obtained: $\bar{T}_{rd,M}$, at not directly irradiated position, and $\bar{T}_{rb,M}$ at irradiated positions.

The difference between the two measured values can be assumed to be only related to direct radiation as long as the following conditions are verified:

- the environment is symmetric, regular and the two measurement points are very close to each other, so that the effects of the diverse view factors in the two points can be neglected;
- the diffuse radiation (both the one directly shining on the globe from the window and the one formerly reflected by the walls of the room) is not shielded in either measurement position and hence it is always present.

These conditions are largely verified in the room where the measures were carried out and therefore, the two mean radiant temperature $\bar{T}_{rd,M}$ and $\bar{T}_{rb,M}$, assessed by means of the globe-thermometer, can be assumed to differ only for the term related to the direct radiation, $\Delta\bar{T}_{rb}^4$, where:

$$\Delta\bar{T}_{rb}^4 = \frac{\alpha_{SW}}{\varepsilon_S \sigma} (f_p I_b + 0.5 \rho_{floor} I_{bh}) \quad (23)$$

Therefore, the reliability of the proposed model in predicting the effect of the direct component of solar radiation may be tested comparing the measured value $\bar{T}_{rb,M}$ with the one calculated by means of the equation:

$$\bar{T}_{rb,C} = \sqrt[4]{\bar{T}_{rd,M}^4 + \Delta\bar{T}_{rb}^4} \quad (24)$$

or, with a greater detail:

$$\bar{T}_{rb,C} = \sqrt[4]{\bar{T}_{rd,M}^4 + \frac{\alpha_{SW}}{\varepsilon_S \sigma} (f_p I_b + 0.5 \rho_{floor} I_{bh})} \quad (25)$$

As a matter of fact, the smaller the difference between the two values $\bar{T}_{rb,M}$ and $\bar{T}_{rb,C}$ is, the more reliable the proposed model proves to be in taking into account the direct component of solar radiation.

Indeed, to allow the application of eqs. (20) and (24), the needed environmental parameters (i.e. air temperature, air velocity solar radiation) were also measured.

As far as solar radiation is concerned the global radiation on the horizontal plane, I_h , was measured; to assess the direct component, I_{bh} , the method of Reindl et al. [42] was exploited. The direct normal radiation, on the other hand, was calculated by means of the equation:

$$I_b = \frac{I_{bh}}{\sin \alpha} \quad (26)$$

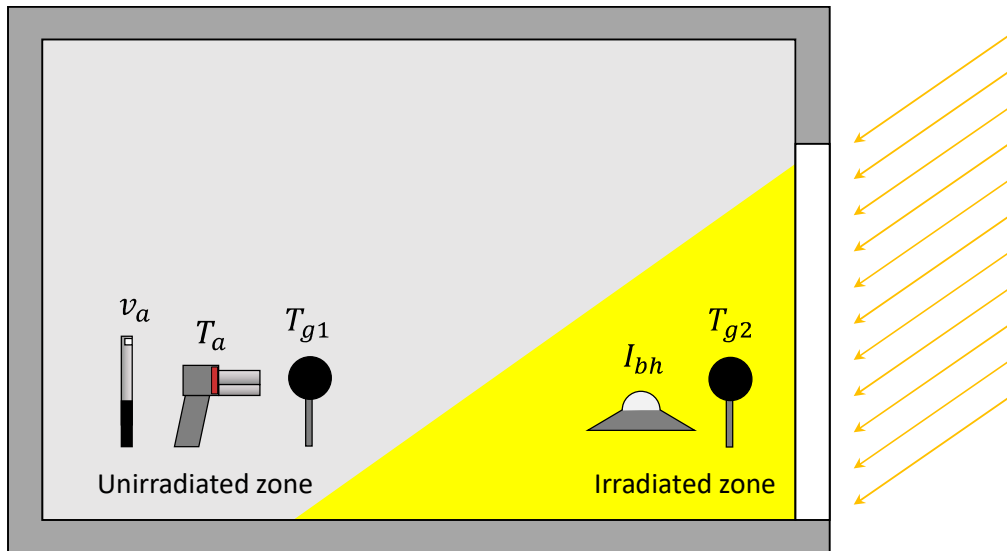
where α is the solar altitude.

To sum up, the following parameters were measured: air temperature (t_a), air velocity (v_a), global solar radiation on the horizontal plane (I_h), directly irradiated globe temperature (T_{gb}), not-directly irradiated globe temperature (T_{gd}); whereas, by means of the equation (20) the directly irradiated ($\bar{T}_{rb,M}$) and not-directly irradiated ($\bar{T}_{rd,M}$) mean radiant temperature were assessed.

On the other hand, using equation (24), the directly irradiated mean radiant temperature ($\bar{T}_{rb,C}$) was also assessed. In this case, the following assumptions were made:

- $\alpha_{sw} = 0.70$ (dimensionless);
- $\varepsilon_s = 0.97$ (dimensionless);
- $\sigma = 5.67 \times 10^{-8} \frac{W}{m^2K^4}$;
- $f_p = \frac{\pi D^2}{4} \times \frac{1}{\pi D^2} = 0.25$, being the projected area factor of the globe-thermometer (dimensionless);
- $\rho_{floor} = 0.5$, taking into account the effect of the long wave radiation generated by the local heating of the portion of the floor surface illuminated by the directed solar beam (dimensionless).

The whole procedure is summarized in Figure 6.



UNIRRADIATED ZONE	IRRADIATED ZONE
<u>Measured Parameters</u>	
v_a T_a T_{g1}	I_{bh} T_{g2}
<u>Preliminary calculations</u>	
$h_{cg} = \max \left\{ 1.4 \sqrt[4]{\frac{T_g - T_a}{D}}; \frac{6.3 v_a^{0.6}}{D^{0.4}} \right\}$	$I_b = \frac{I_{bh}}{\sin \alpha}$
<u>Intermediate calculations</u>	
$\bar{T}_{rd,M} = \sqrt[4]{T_{g1}^4 + \frac{h_{cg1}}{\epsilon_g \sigma} (T_{g1} - T_a)}$	$\Delta \bar{T}_{rb}^4 = \frac{\alpha_{SW}}{\epsilon_S \sigma} (f_p I_b + 0.5 \rho_{floor} I_{bh})$ $\bar{T}_{rb,M} = \sqrt[4]{T_{g2}^4 + \frac{h_{cg2}}{\epsilon_g \sigma} (T_{g2} - T_a)}$
<u>Final calculations</u>	
	$\bar{T}_{rb,C} = \sqrt[4]{\bar{T}_{rd,M}^4 + \Delta \bar{T}_{rb}^4}$ ← COMPARISON

Figure 6 – Procedure used for model validation.

The measures were carried out inside an indoor environment located at the second floor of a building sited in Reggio Calabria (38° 06' 37" North Latitude, 15°39'40" Est Longitude).

The room has only one external wall which is East facing and equipped with a window 1.50 m large and 2.40 m high.

The specifications of the measurements (date, time, room, sampling rates) are reported in Table 1.

Table 1- Specifications of the measurements.

Day	Measurement duration	Sample rate (min)
8 th - July	7:00 – 10:30	5
9 th - July	7:00 – 10:30	5
10 th - July	7:00 – 10:30	5
23 rd - August	7:00 – 10:30	5

3.1 Experimental apparatus

The experimental apparatus is a monitoring system consisting of a set of probes measuring the environmental parameters, connected to the programmable data-logger LSI Babuc A.

The used probes are:

- two globe-thermometer BST131;
- a hot wire anemometer BSV101;
- a psychrometer BSU102;
- a pyranometer BSR153.

The experimental apparatus is depicted in Figure 7 and the technical characteristics of the probes are reported in Table 2.

Table 2- Technical characteristics of the probes.

Measured parameter	Probe type	Probe code	Measurement range	Accuracy	Response time
Air temperature	psychrometer	BSU 102	-5...+60°C	0.10 °C	1.5 min
Air velocity	hot wire anemometer	BSV 101	0.01...20 ms ⁻¹	0...0,5 m/s	0.01 sec
Globe temperature	globe-thermometer	BST 131	-40...+80°C	0.15 °C	20 min
Radiation	pyranometer	BSR 153	0...2000 Wm ⁻²	< 5%	< 30 s

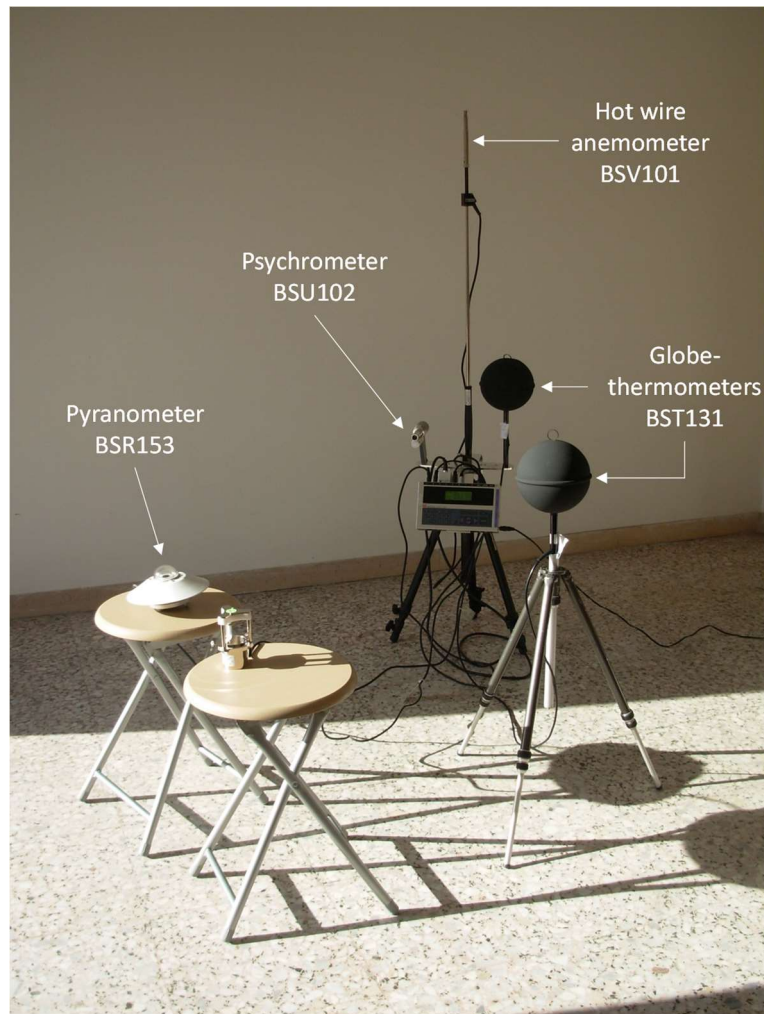


Figure 7 – Experimental apparatus.

As far as the air velocity measurement is concerned, it is worth noting that an unidirectional hot wire anemometer was used. Nevertheless, the particular environmental conditions make the consequent error ineffective in influencing the mean radiant temperature values.

As a matter of fact, the room where the experimental campaign was allocated has no mechanical ventilation equipment and no air conditioning system at all. The air flux regime is ruled by natural convection and the involved air velocities assume very low value (lower than 0.07 m/s) for the whole time.

This fact is true in all the space directions and was verified at the beginning of the experimental campaign measuring, for limited periods of time, the air velocity by positioning the hot wire sensor along with the three spatial directions.

As a consequence, the convective heat transfer coefficient h_{cg} , involved in MRT assessment, is always calculated by means of eq.(21) where there is no dependence on air velocity.

In other words, owing to the features of the natural convection regime characterizing the air movement inside the studied room, the mean radiant temperature does not depend on the air velocity; therefore, the measure of this parameter with the hot wire anemometer was only used to verify the persistence of the described conditions and the consequent error was assumed as negligible, having no influence on the final result which is the calculation of the mean radiant temperature.

However, it should also be highlighted that the used probe is designed to respond to plane omnidirectional air flow which arrive on the hot wire from any directions within 300°.

As a consequence, only the component having the same direction of the hot wire might be lost and, owing to its small value, the correlated error can be assumed as negligible.

3.2 Experimental results

The results of the measurements are reported in Figures 3-5. In this regard, it is worth noticing that the measures were always terminated when, because of the combined effect of time and shadows due to the building structures, the condition $I_h < 50 \text{ W/m}^2$ was verified, which happened after 10:30 on average.

During all the measures, however, the global solar radiation on the horizontal plane never exceeded 750 W/m^2 , which was reached in the morning of the 8th and the 10th of July.

As expected, on the other hand, while the mean radiant temperature measured at points not directly irradiated by the sun, $\bar{T}_{rd,M}$, is slightly affected by solar radiation, the mean radiant temperatures measured in correspondence of directly irradiated positions, $\bar{T}_{rb,M}$, rising up to 65°C and over, appear to depend on the global solar radiation to a large extent.

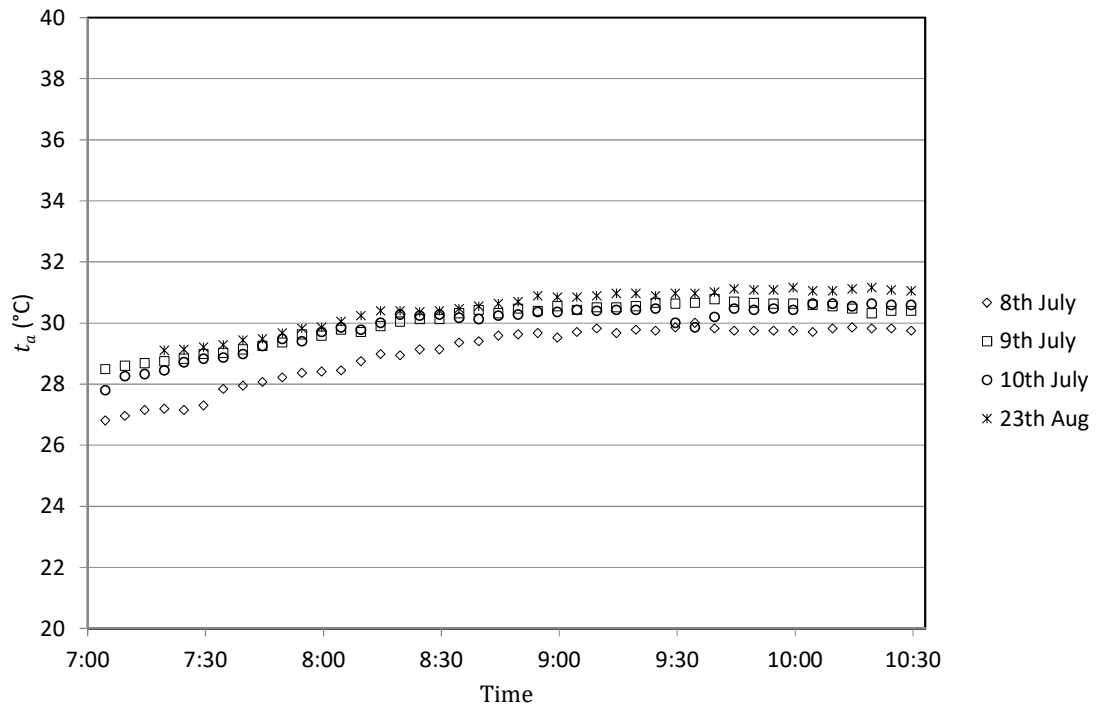


Figure 8 – Measured air temperature.

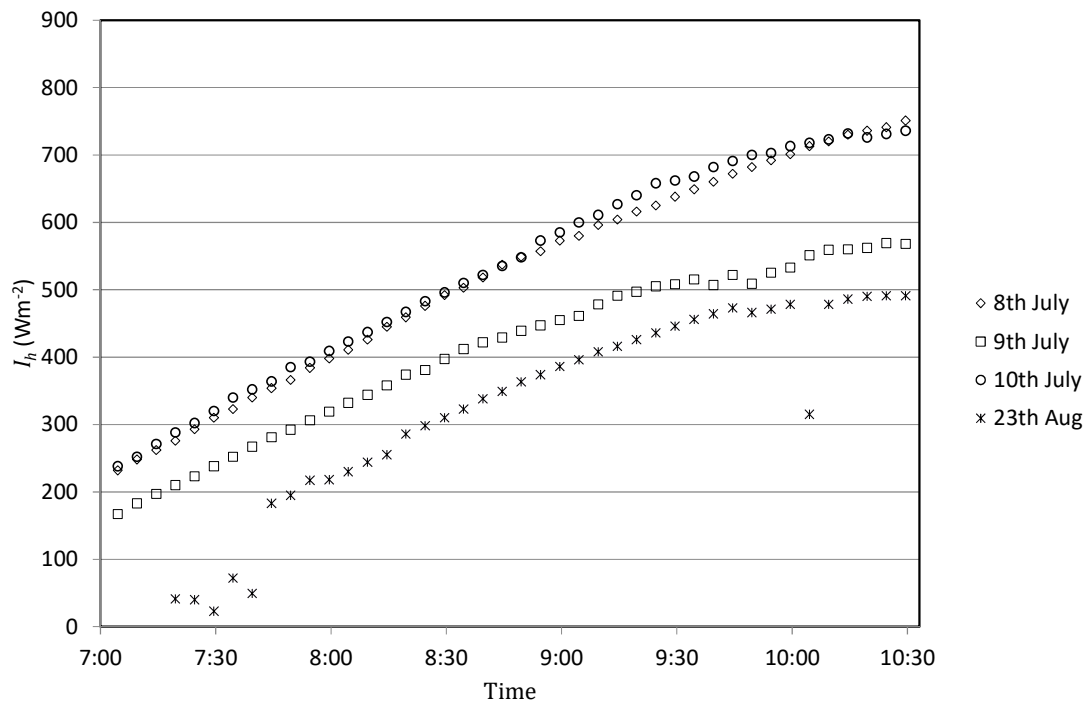


Figure 9 – Measured Solar radiation on the horizontal plane.

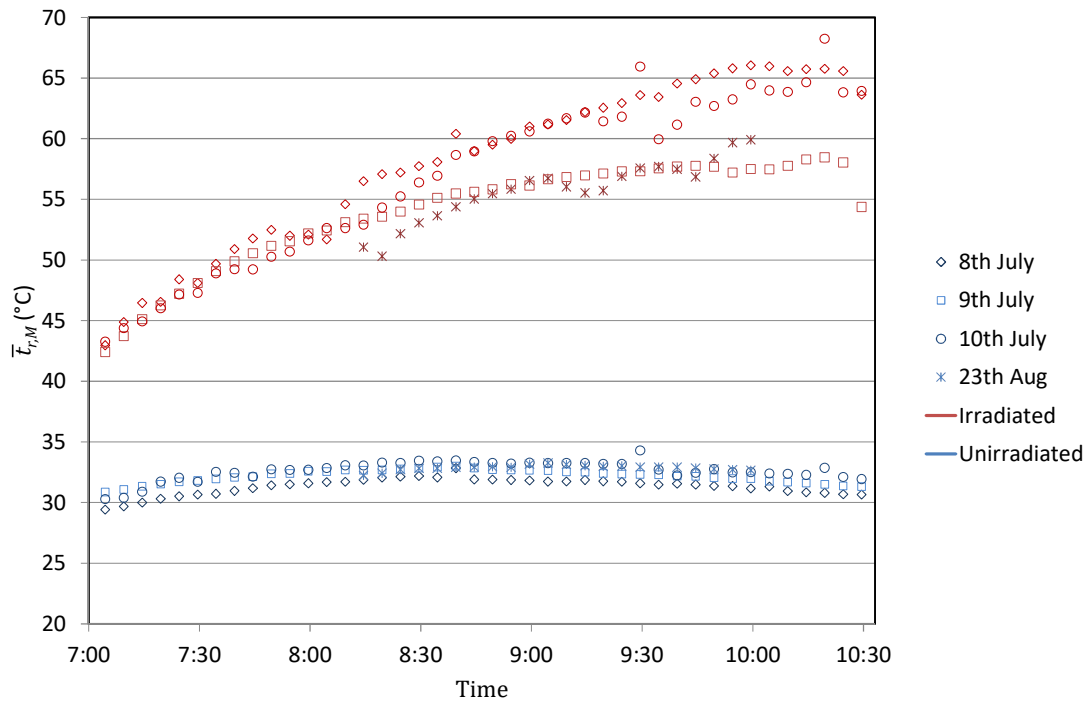


Figure 10 – Mean Radiant temperature.

4 Comparing model predictions with experimental data

A comparison between the two mean radiant temperature $\bar{T}_{r,b,M}$ and $\bar{T}_{r,b,C}$, respectively measured and calculated by eq. (24), is reported in the following figures.

Precisely, in Figure 11 the time trend of the two parameters is depicted, whereas Figure 12, showing the distance among measured and calculated values, allows the appraisal of the accuracy of the proposed model in predicting the effect of the direct component of solar radiation.

The analysis of the data shows that the calculated values are fairly consistent with the completely measured ones. Therefore, from these preliminary results, the term $\Delta \bar{T}_{rb}^4$ seems to predict the effect of the direct component of solar radiation rather suitably.

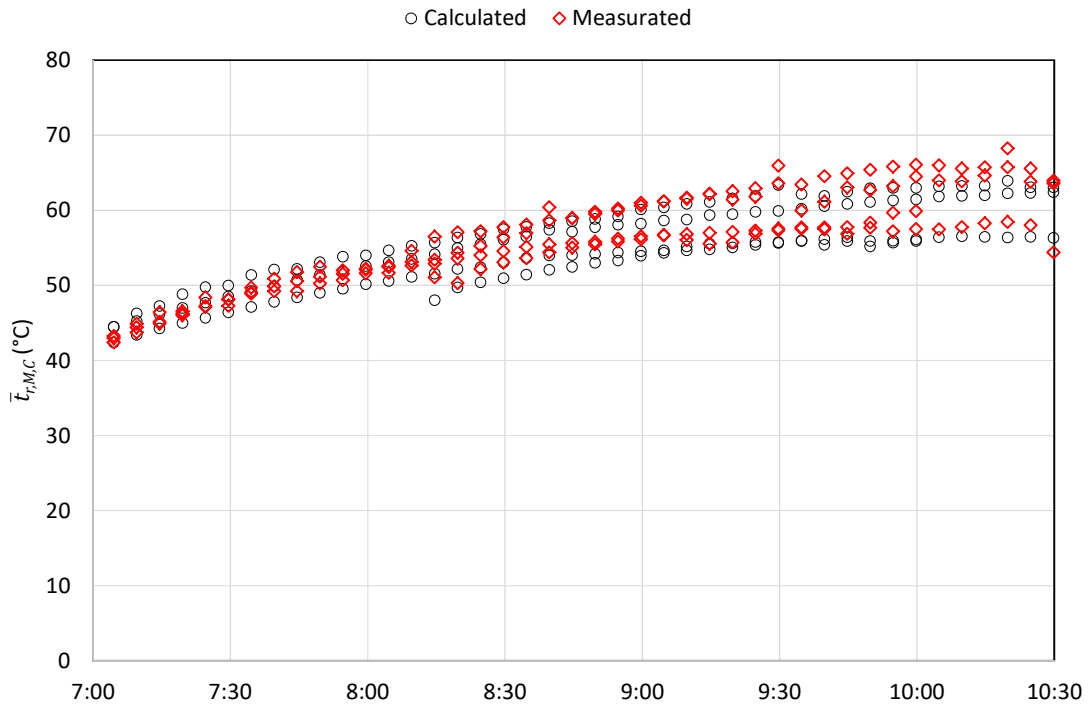


Figure 11 – Time trend of the measured mean radiant temperature, $\bar{t}_{r,b,M}$, and the calculated mean radiant temperature, $\bar{t}_{r,b,C}$, for a subject directly irradiated by the sun.

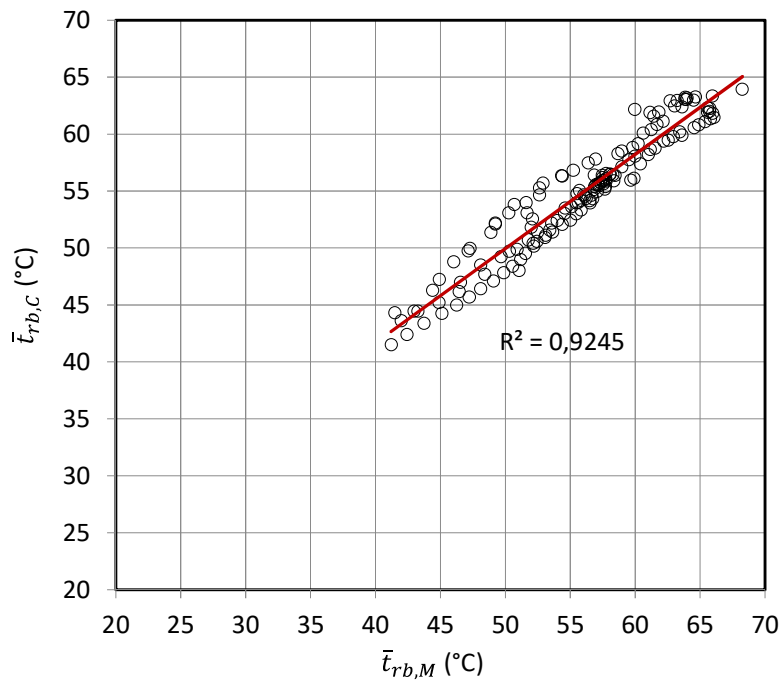


Figure 12 – Comparison among the measured mean radiant temperature, $\bar{t}_{r,b,M}$, and the calculated mean radiant temperature, $\bar{t}_{r,b,C}$, for a subject irradiated by the sun.

The differences also noticeable can be presumably attributed to the fact that the contribute of the diffuse solar radiation is not completely uniform as, on the contrary, it was assumed in order to assess $\bar{t}_{r,b,C}$ by means of eq (24).

Moreover, it must be highlighted that the inertia of the probe could also have a role in causing the differences among measured and calculated values.

Nevertheless, it is also worthy of note that both the model and the experimental results seem to follow similar time trends (Figure 11) and, therefore, the effect of the probe could be effective only to a limited extent. This could be justified by the fact that 5 min average experimental values were used in the comparison phase, so that the effect of rapid changes in the radiation fluxes are inevitably smoothed [18].

Furthermore, at the beginning of every measurement, the data sampling started only after the probe had been exposed to solar radiation for about fifteen minutes at least, so that the experimental results, which were considered for comparison purposes, were not affected by the initial and probably not negligible transitory phenomena.

However, with a view to clarifying this aspect, the future development of the research are being planned in this direction, involving probes with smaller diameter (< 40mm).

On balance, however, at the current stage of the research, the proposed model seems to predict adequately the mean radiant temperature value in presence of solar radiation, and this fact appears to justify further investigations aimed at the measurement of all the radiation components in order to reach a decisive response on this matter. In this direction the future development of the research is planned.

5 Conclusion

The purpose of this paper is to propose a reliable and feasible relationship for the evaluation of the mean radiant temperature for a human subject placed in a confined environment, and irradiated by solar radiation, direct, diffuse and reflected as well.

The application of the proposed algorithm, which allows to take into account the time and space variations of the climatic conditions defining the radiant field, requires the acquaintance with a series of parameters which are definitely assessable: the temperatures of the internal surfaces of the environment; the angle factors among the opaque and glazed surfaces of the environment and the subject; the rate of the diffuse and direct solar radiation entering the room through the glazed surfaces; the reflection coefficients of the indoor surfaces to solar radiation; the angle factors among the glazed and the opaque surfaces of the environment; the projected area factors of the subject in the solar beam direction.

To sum up, the method is designed to realize a detailed evaluation of the mean radiant temperature which can be, in turn, exploited for thermal comfort optimization and energy efficiency purposes, allowing an optimal sizing and management of systems within the constraints defined by the comfort conditions.

Moreover, in order to try to investigate the real effects of solar radiation, a series of experimental measures were carried out. They were specifically designed to analyze the effect of the direct solar component on the mean radiant temperature and to validate the predictions of the proposed model in this regard. As expected, the mean radiant temperature proved to be highly affected by solar irradiance and the proposed model seems to predict this behavior rather satisfactorily.

As a matter of fact, notwithstanding the inertia of the probe could have a role in causing the detected discrepancies, the model predictions and the measured data follow similar time trend and the differences among the calculated and measured values are relatively small. This behavior could be explained on account of the fact that 5 min average experimental values were used in the comparison phase, so that the influence of the time variability of the radiative flux is reduced.

In conclusion, the described preliminary experimental results show that the proposed model seems to predict adequately the mean radiant temperature value in presence of solar radiation, albeit particular occurrences seem to prove the need of further investigation on this topic. In this direction the future development of the research is planned.

Nomenclature

A_i	area of the i^{th} surface of the envelope [m ²]
A_E	whole area of the surface of the envelope [m ²]
A_p	projected area of the subject onto a plain normal to the direction of the solar beam [m ²]
A_S	effective area of the human body exposed to radiation [m ²]
D	globe-thermometer diameter [m]
$\Delta\bar{T}_{rb}$	contribution to the mean radiant temperature due to the direct component of the solar radiation [K]
f_p	projected area factor
$F_{j \rightarrow i}$	angle factor between the j^{th} glazed surface and the i^{th} surface of the envelope
$F_{S \rightarrow j}$	angle factor between the subject and the j^{th} glazed surface of the envelope
h_{cg}	convective heat transfer coefficient [Wm ⁻² K ⁻¹]

I_b	direct solar radiation that strikes the subject [Wm^{-2}]
I_{bh}	direct solar radiation on the horizontal plane [Wm^{-2}]
I_{dj}	diffuse sky radiation entering the room through the j^{th} glazed surface [Wm^{-2}]
I_h	global solar radiation on the horizontal plane [Wm^{-2}]
Q_{0S}	emitted flow [W]
$Q_{A \rightarrow S}$	radiative flux emitted by the surfaces of the environment [W]
$Q_{B \rightarrow S}$	short wave solar radiant flux on the body surface, entering the room through the glazed surface and due to the direct radiation [W]
$Q_{D \rightarrow S}$	short wave solar radiant flux on the body surface, entering the room through the glazed surface and due to the diffuse sky radiation [W]
$Q_{E \leftrightarrow S}$	flux exchanged for radiation among the human body and the surfaces of the environment [W]
Q_S	net flux leaving the human body [W]
$Q_{S,abs}$	absorbed share of the thermal flow that reaches the subject [W]
T_a, t_a	air temperature [K, °C]
T_{cl}	mean temperature of clothed surface [K]
T_g, t_g	globe-thermometer temperature [K, °C]
T_{gd}, t_{gd}	globe temperature, in not directly irradiated position [K, °C]
T_{gb}, t_{gb}	globe temperature, in irradiated position [K, °C]
T_i	temperature of the i^{th} surface of the envelope [K]
\bar{T}_r, \bar{t}_r	mean radiant temperature [K, °C]
$\bar{T}_{rb,C}, \bar{t}_{rb,C}$	calculated mean radiant temperature, in the presence of the direct component of the solar radiation [K, °C]
$\bar{T}_{rb,M}, \bar{t}_{rb,M}$	measured mean radiant temperature, considering the effect of the direct component of the solar radiation [K, °C]
$\bar{T}_{r,C}, \bar{t}_{r,C}$	calculated mean radiant temperature [K, °C]
\bar{T}_{rd}	mean radiant temperature, without considering the direct component of the solar radiation [K]
$\bar{T}_{rd,M}$	measured mean radiant temperature, without considering the effect of direct component of the solar radiation [K]
$\bar{T}_{r,M}$	measured mean radiant temperature [K]
v_a	air velocity [ms^{-1}]
<i>Greek symbols</i>	
α	solar altitude [°]
α_{LW}	long wave absorbance of the human body

α_{SW}	short wave absorbance of the human body
ε_g	emissivity of the globe-thermometer
ε_s	emissivity of the human body
ε_E	emissivity of the surfaces of the environment
ρ_i	reflectance of the i^{th} surface of the envelope
ρ_{floor}	reflectance of the pavement
σ	Stefan–Boltzmann constant($5,67 \times 10^{-8} \text{ Wm}^{-2}\text{K}^{-4}$)

References

- [1] F. Calvino, M. La Gennusa, M. Morale, G. Rizzo, G. Scaccianoce, Comparing different control strategies for indoor thermal comfort aimed at the evaluation of the energy cost of quality of building, *Appl. Therm. Eng.* 30 (2010) 2386–2395. doi:10.1016/j.applthermaleng.2010.06.008.
- [2] C. Marino, A. Nucara, G. Peri, M. Pietrafesa, A. Pudano, G. Rizzo, An MAS-based subjective model for indoor adaptive thermal comfort, *Sci. Technol. Built Environ.* 21 (2015) 114–125. doi:10.1080/10789669.2014.980683.
- [3] C. Marino, A. Nucara, M. Pietrafesa, Proposal of comfort classification indexes suitable for both single environments and whole buildings, *Build. Environ.* 57 (2012) 58–67. doi:10.1016/j.buildenv.2012.04.012.
- [4] CEN, EN 15251 - Indoor environmental input parameters for design and assessment of energy performance of buildings- addressing indoor air quality, thermal environment, lighting and acoustics, (2007).
- [5] ISO, ISO 7730 - Ergonomics of the thermal environment - Analytical determination and interpretation of thermal comfort using calculation of the PMV and PPD indices and local thermal comfort criteria, International Standard Organization, Geneva, 2005.
- [6] M. Dell’Isola, A. Frattolillo, B.I. Palella, G. Riccio, Influence of measurement uncertainties on the thermal environment assessment, *Int. J. Thermophys.* 33 (2012) 1616–1632. doi:10.1007/s10765-012-1228-7.
- [7] F.R. D’Ambrosio Alfano, B.W. Olesen, B.I. Palella, G. Riccio, Thermal comfort: Design and assessment for energy saving, *Energy Build.* 81 (2014) 326–336. doi:10.1016/j.enbuild.2014.06.033.
- [8] M. La Gennusa, A. Nucara, G. Rizzo, G. Scaccianoce, The calculation of the mean radiant temperature of a subject exposed to the solar radiation—a generalised algorithm, *Build. Environ.* 40 (2005) 367–375. doi:10.1016/j.buildenv.2004.06.019.
- [9] C. Marino, A. Nucara, M. Pietrafesa, Mapping of the indoor comfort conditions considering the effect of solar radiation, *Sol. Energy.* 113 (2015) 63–77. doi:10.1016/j.solener.2014.12.020.
- [10] K.C. Parsons, *Thermal Environments: The Effects of Hot, Moderate, and Cold Environments*

on Human Health, 3rd ed., Taylor & Francis, Boca Raton, 2014.

- [11] F. Lindberg, B. Holmer, S. Thorsson, SOLWEIG 1.0 – Modelling spatial variations of 3D radiant fluxes and mean radiant temperature in complex urban settings, *Int. J. Biometeorol.* 52 (2008) 697–713. doi:10.1007/s00484-008-0162-7.
- [12] J. Huang, J.G. Cedeño-Laurent, J.D. Spengler, CityComfort+: A simulation-based method for predicting mean radiant temperature in dense urban areas, *Build. Environ.* 80 (2014) 84–95. doi:10.1016/j.buildenv.2014.05.019.
- [13] N. Kántor, J. Unger, The most problematic variable in the course of human-biometeorological comfort assessment — the mean radiant temperature, *Cent. Eur. J. Geosci.* 3 (2011) 90–100. doi:10.2478/s13533-011-0010-x.
- [14] E.L. Krüger, F.O. Minella, A. Matzarakis, Comparison of different methods of estimating the mean radiant temperature in outdoor thermal comfort studies., *Int. J. Biometeorol.* 58 (2014) 1727–37. doi:10.1007/s00484-013-0777-1.
- [15] N. Kántor, T.-P. Lin, A. Matzarakis, Daytime relapse of the mean radiant temperature based on the six-directional method under unobstructed solar radiation, *Int. J. Biometeorol.* 58 (2014) 1615–1625. doi:10.1007/s00484-013-0765-5.
- [16] N. Kántor, J. Unger, The most problematic variable in the course of human-biometeorological comfort assessment — the mean radiant temperature, *Cent. Eur. J. Geosci.* 3 (2011) 90–100. doi:10.2478/s13533-011-0010-x.
- [17] C.L. Tan, N.H. Wong, S.K. Jusuf, Effects of vertical greenery on mean radiant temperature in the tropical urban environment, *Landsc. Urban Plan.* 127 (2014) 52–64. doi:10.1016/j.landurbplan.2014.04.005.
- [18] S. Thorsson, F. Lindberg, I. Eliasson, B. Holmer, Different methods for estimating the mean radiant temperature in an outdoor urban setting, in: *Int. J. Climatol.*, John Wiley & Sons, Ltd., 2007: pp. 1983–1993. doi:10.1002/joc.1537.
- [19] F.R. d’Ambrosio Alfano, M. Dell’Isola, B.I. Palella, G. Riccio, A. Russi, On the measurement of the mean radiant temperature and its influence on the indoor thermal environment assessment, *Build. Environ.* 63 (2013) 79–88. doi:10.1016/j.buildenv.2013.01.026.
- [20] I. Atmaca, O. Kaynakli, A. Yigit, Effects of radiant temperature on thermal comfort, *Build. Environ.* 42 (2007) 3210–3220. doi:10.1016/j.buildenv.2006.08.009.
- [21] M.C. Singh, S.N. Garg, R. Jha, Different glazing systems and their impact on human thermal comfort-Indian scenario, *Build. Environ.* 43 (2008) 1596–1602. doi:10.1016/j.buildenv.2007.10.004.
- [22] A. Tzempelikos, M. Bessoudo, A.K. Athienitis, R. Zmeureanu, Indoor thermal environmental conditions near glazed facades with shading devices – Part II: Thermal comfort simulation and impact of glazing and shading properties, *Build. Environ.* 45 (2010) 2517–2525. doi:10.1016/j.buildenv.2010.05.014.
- [23] M. Bessoudo, A. Tzempelikos, A.K. Athienitis, R. Zmeureanu, Indoor thermal environmental conditions near glazed facades with shading devices – Part I: Experiments and building

thermal model, *Build. Environ.* 45 (2010) 2506–2516. doi:10.1016/j.buildenv.2010.05.013.

- [24] D.H. Kang, P.H. Mo, D.H. Choi, S.Y. Song, M.S. Yeo, K.W. Kim, Effect of MRT variation on the energy consumption in a PMV-controlled office, *Build. Environ.* 45 (2010) 1914–1922. doi:10.1016/j.buildenv.2010.02.020.
- [25] EU, Directive 2010/31/EU of The European Parliament and of the Council of 19 May 2010 on the energy performance of buildings (recast), (2010). <http://eur-lex.europa.eu/LexUriServ/LexUriServ.do?uri=OJ:L:2010:153:0013:0035:EN:PDF>.
- [26] EU, Directive 2002/91/EC of the European Parliament and of the Council of 16 December 2002 on the energy performance of buildings, (2003).
- [27] USA Congress, Energy Policy Act of 2005, Public Law 109–58—Aug. 8, 2005, (2005). <https://www.gpo.gov/fdsys/pkg/PLAW-109publ58/pdf/PLAW-109publ58.pdf>.
- [28] R. of China, Renewable Energy Law of the People’s Republic of China, (2005). <http://english.mofcom.gov.cn/article/policyrelease/Businessregulations/201312/20131200432160.shtml>.
- [29] S.G. Hodder, K. Parsons, The effects of solar radiation on thermal comfort, *Int. J. Biometeorol.* 51 (2006) 233–250. doi:10.1007/s00484-006-0050-y.
- [30] E. Arens, T. Hoyt, X. Zhou, L. Huang, H. Zhang, S. Schiavon, Modeling the comfort effects of short-wave solar radiation indoors, *Build. Environ.* 88 (2015) 3–9. doi:10.1016/j.buildenv.2014.09.004.
- [31] M. La Gennusa, A. Nucara, M. Pietrafesa, G. Rizzo, A model for managing and evaluating solar radiation for indoor thermal comfort, *Sol. Energy.* 81 (2007) 594–606. doi:10.1016/j.solener.2006.09.005.
- [32] F. Kreith, R.M. Manglik, M.S. Bohn, Principles of Heat Transfer, 7th Editio, Cengage Learning, Inc, Stamford, CT 06902 USA, 2011.
- [33] ISO, ISO 7726 - Ergonomics of the thermal environment - Instruments for measuring physical quantities, International Standard Organization, Geneva, 1998.
- [34] P.O. Fanger, Thermal comfort, Danish Technical Press, Copenhagen, 1970.
- [35] ASHRAE, ASHRAE Handbook - HVAC Applications, American Society of Heating, Refrigerating and Air-Conditioning Engineers, Inc. Atlanta, GA, 1989.
- [36] M. La Gennusa, A. Nucara, M. Pietrafesa, G. Rizzo, G. Scaccianoce, Angle Factors and Projected Area Factors for Comfort Analysis of Subjects in Complex Confined Enclosures: Analytical Relations and Experimental Results, *Indoor Built Environ.* 17 (2008) 346–360. doi:10.1177/1420326X08094621.
- [37] F. Calvino, M. La Gennusa, A. Nucara, G. Rizzo, G. Scaccianoce, Evaluating human body area factors from digital images: A measurement tool for a better evaluation of the ergonomics of working places, *Occup. Ergon.* 5 (2005) 173–185.
- [38] G. Rizzo, G. Franzitta, G. Cannistraro, Algorithms for the calculation of the mean projected area factors of seated and standing persons, *Energy Build.* 17 (1991) 221–230.

doi:10.1016/0378-7788(91)90109-G.

- [39] G. Rizzo, G. Cannistraro, G. Franzitta, Algorithms for the calculation of the view factors between persons and rectangular surfaces in parallelepiped environments, *Energy Build.* 19 (1992) 51–60. doi:10.1016/0378-7788(92)90035-F.
- [40] M. La Gennusa, G. Rizzo, G. Scaccianoce, A. Nucara, Radiative heat exchanges of people in complex geometry buildings: An experimentally based algorithm for computing angle factors, in: 44th Annu. Hum. Factors Ergon. Soc. Aust. Conf. 2008, HFESA 2008, 2008: pp. 69–76.
- [41] G. Rizzo, G. Cannistraro, G. Franzitta, Algorithms for the calculation of the view factors between persons and rectangular surfaces in parallelepiped environments, *Energy Build.* 19 (1992) 51–60. doi:10.1016/0378-7788(92)90035-F.
- [42] D.T. Reindl, W.A. Beckman, J.A. Duffie, Diffuse fraction correlations, *Sol. Energy.* 45 (1990) 1–7. doi:10.1016/0038-092X(90)90060-P.